metabolism. Thus from the standpoint of examining bone mass questions, well-matched normal women are appropriate controls for this study.

It is noteworthy that our patients started the study with greater mean bone density than did the controls. This observation may simply reflect normal variation in initial bone mass in a small series of women. It is possible, however, that the greater initial bone mass of the patients implied an increased degree of endogenous estrogenization, compared with healthy controls, thereby predisposing the patients to the development of breast carcinoma. One study of patients with breast cancer has shown a positive relationship between bone mineral content and the amount of tumor tissue estrogen receptors, the latter receptors providing a possible measurement of estrogen effect in the patients (*26*).

In summary, we found preservation of bone mineral density in postmenopausal patients with breast cancer during the first year of tamoxifen treatment, whereas healthy postmenopausal controls experienced a predictable and significant loss of spinal bone mineral over the same amount of time. If larger, more long-term studies bear out these preliminary findings, concerns about accelerated bone mineral loss in tamoxifen-treated postmenopausal breast cancer patients may be resolved. Moreover, tamoxifen may prove to be beneficial in the treatment of postmenopausal osteoporosis in a selected population of normal women for whom estrogen supplementation may be contraindicated.

References

(*1*) KIANG DT, KENNEDY BJ: Tamoxifen (antiestrogen) therapy in advanced breast cancer. Ann Intern Med 87:687-690, 1977

(*2*) FISHER B, REDMOND C, BROWN A, ET AL: Treatment of primary breast cancer with chemotherapy and tamoxifen. N Engl J Med 305:1-6, 1981

(*3*) TERENIUS L: Structure-activity relationships of anti-oestrogens with regard to interaction with 17β-oestradiol in the mouse uterus and vagina. Acta Endocrinol 66:431-447, 1971

(*4*) SUTHERLAND R, MESTER J, BAULIER EE: Tamoxifen is a potent "pure" anti-estrogen in chick oviduct. Nature 267:434-437, 1977

(*5*) JORDAN VC, DIX CJ, NAYLOR KE, ET AL: Non-steroid antiestrogens: Their biological effects and potential mechanisms of action. J Toxicol Environ Health 4:363-390, 1978

(*6*) KATZENELLENBOGEN BS, BHAKOO HS, FERGUSON ER, ET AL: Estrogen and antiestrogen action in reproductive tissues and tumors. Recent Prog Horm Res 35:259-292, 1979

(*7*) JORDAN VC: Biochemical pharmacology of antiestrogen action. Pharmacol Rev 36:245-276, 1984

(*8*) STEWART PJ, STERN PH: Effects of the antiestrogens tamoxifen and clomiphene on bone resorption in vitro. Endocrinology 118:125-131, 1986

(*9*) TURNER RT, WAKLEY GK, HANNON KS, ET AL: Tamoxifen prevents the skeletal effects of ovarian hormone deficiency in rats. J Bone Miner Res 2:449-456, 1987

(*10*) TURNER RT, WAKLEY GK, HANNON KS, ET AL: Tamoxifen inhibits osteoclast-mediated resorption of trabecular bone in ovarian hormone-deficient rats. Endocrinology 122:1146-1150, 1988

(*11*) JORDAN VC, PHELPS E, LINDGREN JU: Effects of anti-estrogens on bone in castrated and intact female rats. Breast Cancer Res Treat 10:31-35, 1987

(*12*) LOVE R, MAZESS DC, TORMEY P, ET AL: Bone mineral density (BMD) in women with breast cancer treated with tamoxifen for two years. Breast Cancer Res Treat 10:12, 1987

(*13*) BEALL PT, MISRA LK, YOUNG RL, ET AL: Clomiphene protects against osteoporosis in the mature ovariectomized rat. Calcif Tissue Int 36:123-125, 1984

(*14*) AL-AZZAWI F, HART DM, LINDSAY R: Long term effect of oestrogen replacement therapy on bone mass as measured by dual photon absorptiometry. Br Med J 294:1261-1262, 1987

(*15*) AITKEN JM, HART DM, LINDSAY R: Oestrogen replacement therapy for prevention of osteoporosis after oophorectomy. Br Med J 2:515-518, 1973

(*16*) WEISBRODE SE, CAPEN CC: The ultrastructural effect of estrogens on bone cells in thyroparathyroidectomized rats. Am J Pathol 87:311-322, 1977

(*17*) LINDSAY R, MACLEAN A, KRASZEWSKI A, ET AL: Bone response to termination of oestrogen treatment. Lancet 1:1325-1327, 1978

(*18*) GRAY TK, FLYNN TC, GRAY KM, ET AL: 17β-Estradiol acts directly on the clonal osteoblast cell line UMR 106. Proc Natl Acad Sci USA 84:6267-6271, 1987

(*19*) KOMM BS, TERPENING CM, BENZ DJ, ET AL: Estrogen binding, receptor mRNA, and biologic response in osteoblast-like osteosarcoma cells. Science 241:81-84, 1988

(*20*) ERIKSEN EF, COLVARD DS, BERG NJ, ET AL: Evidence of estrogen receptors in normal human osteoblast-like cells. Science 241:84-86, 1988

(*21*) NUTIK G, CRUESS RL: Estrogen receptors in bone. An evaluation of the uptake of estrogen into bone cells. Proc Soc Exp Biol Med 146:265-268, 1974

(*22*) CAPUTO CB, MEADOWS D, RAISZ LG: Failure of estrogens and androgens to inhibit bone resorption in tissue culture. Endocrinology 98:1065-1068, 1976

(*23*) LISKOVA M: Influence of estrogens on bone resorption in organ culture. Calcif Tissue Res 22:207-218, 1976

(*24*) VAN PAASSEN HC, POORTMAN J, BORGART-CREUTZBURG JHH, ET AL: Oestrogen binding proteins in bone cell cytosol. Calcif Tissue Res 25:249-254, 1978

(*25*) ARNETT R, LINDSAY R, DEMPSTER D: Effect of estrogen and anti-estrogen on osteoclast activity in vitro. J Bone Miner Res 1(suppl):99, 1986

(*26*) NIELSEN HE, POULSON HS, OLSEN KJ, ET AL: Bone mineral content and estrogen receptors in patients with breast cancer. Eur J Cancer Clin Oncol 15:703-707, 1979

Display and Analysis of Patterns of Differential Activity of Drugs Against Human Tumor Cell Lines: Development of Mean Graph and COMPARE Algorithm

K. D. Paull, R. H. Shoemaker, L. Hodes, A. Monks, D. A. Scudiero, L. Rubinstein, J. Plowman, M. R. Boyd*

The objective of this study was to develop and investigate an approach to optimally detect, rank, display, and analyze patterns of differential growth inhibition among cultured cell lines. Such patterns of cellular responsiveness are produced by substances tested in vitro against disease-oriented panels of human tumor cell lines in a new anticancer screening model under development by the National Cancer Institute. In the first phase of the study, we developed a key methodological tool, the mean graph, which allowed the transformation of the numerical cell line response data into graphic patterns. These patterns were particularly expressive of differential cell growth inhibition and were conveniently amenable to further analyses by an algorithm we devised and implemented in the COMPARE computer program. [J Natl Cancer Inst 81:1088-1092, 1989]

Received November 7, 1988; revised March 23, 1989; accepted April 4, 1989.

K. D. Paull, R. H. Shoemaker, L. Hodes, L. Rubinstein, J. Plowman, M. R. Boyd, Developmental Therapeutics Program, Division of Cancer Treatment, National Cancer Institute, National Institutes of Health, Bethesda, MD.

A. Monks, D. A. Scudiero, Program Resources Inc., NCI-Frederick Cancer Research Facility, Frederick, MD.

**Correspondence to:* Dr. K. D. Paull, Developmental Therapeutics Program, National Cancer Institute, NIH, Executive Plaza North, Rm. 831, Bethesda, MD 20892.

The National Cancer Institute (NCI) is implementing a new anticancer drug-screening program using a disease-oriented panel of cultured human tumor cell lines for the initial stages of screening. More detailed aspects of this program and its origins, goals, methods, techniques, and rationale were described previously (*1-4*). Criteria to define activity in the new screen are being explored. One criterion under study, differential cell growth inhibition, was the principal focus of our study.

Differential growth inhibition as defined here means that a cell line or group of cell lines can be inhibited to a given extent at a lower concentration of test drug than is required to exert the same effect on other cell lines. Differential growth inhibition has not been systematically investigated as a criterion for new drug selection. Therefore, unique data treatment and display methods were necessary for examination of its potential for determining activity in the new NCI drug screen. The objective of this study was development of methods to optimally detect, rank, and display test results that signal differential growth inhibition. A key result of the first phase of the study, the mean graph, has catalyzed development of additional methods by transforming the numerical cell line response data into graphic patterns that express differential growth inhibition.

Methods

We performed dose-response testing with cells from each cell line in a pilot screening panel. This panel consisted of ≈50 cell lines, including colon, lung, ovarian, and renal carcinoma; melanoma; central nervous system tumors; human leukemia; and a miscellaneous group of cell lines including the MCF-7 breast cancer and P388 murine leukemia cell lines and multidrug-resistant variants of these two lines. Test samples were prepared in dimethyl sulfoxide at their maximum soluble concentrations, diluted 1:200 with medium, and tested in culture at five $\log_{10}$ dilutions.

Drug screening was performed with automated assay methods described previously (*2,3*). It is important to note that use of a different assay method or end point determination could yield substantively different screening data profiles and interpretations. Nevertheless, our general approach to data display and analysis may be applicable to a variety of assays and/or end points.

Results and Discussion

The large amount of data generated for each compound (≈50 dose-response curves) required an optimal format for the graphic presentation of differential cell growth inhibition. The mean graph format developed for this purpose not only permits the ready visualization of any differential growth inhibition expressed by a test compound but also creates a framework for logical analysis of the data. This framework provides the foundation for computer-assisted analysis of the data, a vital development, considering the unprecedented scale of the NCI in vitro drug-screening program. However, the most intriguing property of the mean graph format is that it yields identifiable and characteristic "fingerprint" patterns, which appear to possess a remarkable degree of structure-function information.

Mean Graph

The concept for the mean graph emerged in part from attempts to detect differential growth inhibition from a standard bar graph presentation. Indications of differential growth inhibition in a standard bar graph format reside only in the "ragged edge," the region between the tips of the bars for the least responsive cell line and the most responsive cell line. Figure 1 illustrates a typical horizontal bar graph and the corresponding mean graph. In this horizontal bar graph, the lengths of the bars are directly proportional to the potency of the test compound against the tumor cell line, which is expressed as the logarithm of the concentration resulting in 50% growth inhibition (IC_{50}). The region between the baseline and the right end of the bar representing the least potent response (fig. 1A) tends to defeat the perception of differential growth inhibition. As an alternative, we developed a graph centered at the arithmetic mean of the logarithm of the IC_{50} values for all cell line responses measured for a compound. While choice of the mean as an anchor point is arbitrary, its use has proven to be advantageous for the development of other mean-graph-derived analyses such as the estimation of relative cell line sensitivities (*5*).

The mean graph (fig. 1C) is constructed by projecting bars to the right or left of the mean, depending on whether cell sensitivity to a test drug is more or less than average. The length of a bar is proportional to the difference between the logarithm of the cell line IC_{50} and the mean. Differential growth inhibition is depicted by the bar (delta), which projects to either side of the mean. A bar projecting 3 log units to the right of the mean, for example, would reflect a cellular response 1,000 times more sensitive than the average of all of the cellular responses to the compound represented on the graph.

Ranking by Degree of Differential Growth Inhibition

One approach to surveillance of the drug-screening data base is to rank compounds by their degree of differential growth inhibition. A novel technique for ranking follows from the mean graph format.

The first step in this approach is to identify a single best delta for a compound among all the deltas generated for it. This best delta is identified as Delta. The simplest definition of Delta is the highest numerical value of delta. However, a potentially better definition of the best delta is that delta representing the largest number of standard deviations from the mean of all the deltas observed for a cell line. Thus, Delta is the statistically rarest delta. The advantage of this statistical approach is that it helps to reduce the selection bias toward the intrinsically more sensitive cell lines. To obtain Delta by this method, one calculates the number of standard deviations from the mean of deltas that each delta represents.

The cell line-specific mean of delta values and the corresponding standard deviations are computed from the delta values for each cell line for all of the compounds evaluated. For a given delta, the appropriate mean is subtracted from the delta, and this differ-

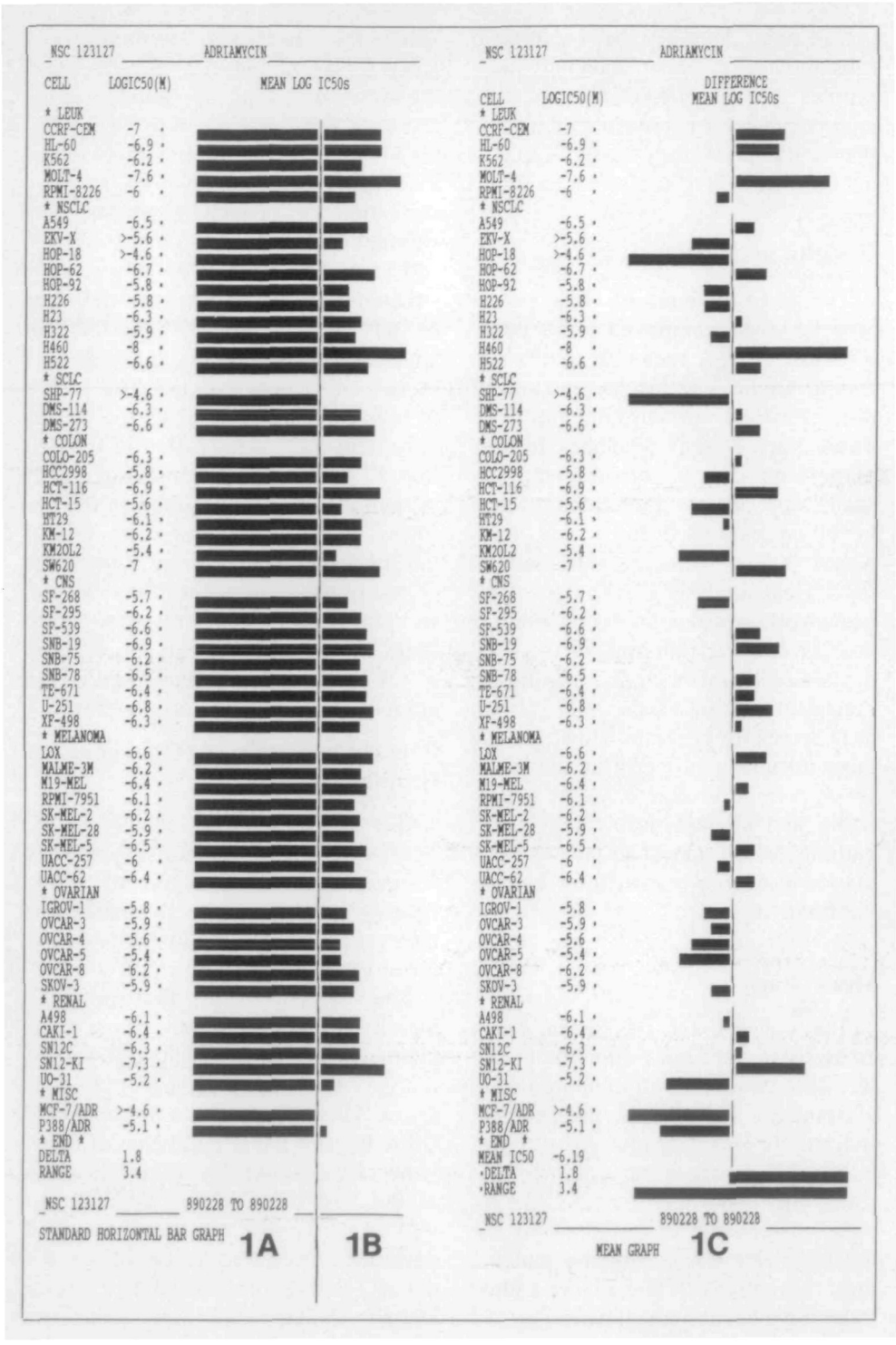

Figure 1. Comparison of two display formats for perception of differential growth inhibition in disease-oriented human tumor cell line panel. In standard horizontal bar graph (left), display of differential drug effects is confined to "ragged edge" (1B). Ready perception of differential effects in section 1B is effectively defeated by presence of large base section, 1A. Mean graph format, section 1C (right), facilitates perception of differential responses of cell lines by eliminating base section and projecting bars in opposite directions depending on whether cell sensitivity to the drug is more or less than average. Resulting fingerprint patterns provide delta values used in COMPARE (pattern-recognition) analyses. LEUK = leukemia; NSCLC = non-small cell lung cancer; SCLC = small cell lung cancer; CNS = central nervous sytem; and MISC = miscellaneous. Range = No. of log units between values for most sensitive and least sensitive cell lines.

ence is divided by the corresponding standard deviation. The quotient is the number of standard deviations from the cell line-specific mean. The means and standard deviations for each cell line are listed in table 1.

The second step in this method is to rank compounds in order of their differential growth inhibition using the Deltas selected in the first step. Searching and sorting by Deltas provides an efficient means to identify compounds exhibiting differential growth inhibition.

Pattern-Recognition Algorithm

Another application of the mean graph format relates to pattern recognition. This format creates a characteristic fingerprint pattern for each compound. The possibility that these patterns might contain other exploitable information was investigated. We devised a simple algorithm that was implemented in the COMPARE computer program to rank the similarity of the mean graph pattern of a specified "seed" compound to the patterns of all the other compounds in the NCI screening project data base. Any previously tested compound can be used as the seed to initiate the pattern-recognition program.

The COMPARE program evaluates the similarity of mean graph patterns by computing average differences be-

Table 1. Cell line-specific means, standard deviations, and confidence limits of delta*

Cell line	Mean	SD	99.96% Confidence limits	No. of delta values
SK-MEL-2	−0.044	0.332	1.116	908
RPMI-7951	0.034	0.336	1.210	871
LoVo	0.032	0.359	1.288	855
SW620	0.084	0.364	1.358	882
NCI-H23	0.049	0.365	1.326	901
NCI-H460	0.000	0.377	1.321	905
DMS-114	0.085	0.392	1.457	833
HT29	−0.088	0.393	1.287	897
H69	0.077	0.394	1.455	794
NCI-H125	0.051	0.396	1.438	866
WiDr	0.049	0.398	1.443	461
SK-MEL-5	0.063	0.399	1.460	876
NCI-H146	0.028	0.401	1.431	713
SN12-KI	−0.006	0.405	1.412	712
DLD-1	−0.124	0.406	1.299	912
OVCAR-3	−0.019	0.407	1.406	658
Malme-3M	0.014	0.408	1.443	893
NCI-H524	0.030	0.417	1.489	764
U-251	0.065	0.421	1.537	824
A549	−0.100	0.422	1.376	914
OVCAR-5	−0.117	0.432	1.396	578
NCI-H522	0.143	0.434	1.663	859
CCRF-CEM	0.276	0.434	1.796	734
SNB44	−0.097	0.440	1.442	716
TE671	0.048	0.443	1.599	874
OVCAR-4	−0.186	0.444	1.369	725
A2780	0.192	0.444	1.748	800
MCF-7	−0.062	0.447	1.504	896
SNB-19	−0.053	0.447	1.513	797
K562	0.132	0.448	1.698	867
NCI-H82	0.163	0.450	1.738	767
HCC2998	−0.129	0.453	1.455	534
SK-MES-1	0.036	0.460	1.647	575
A498	−0.002	0.465	1.627	711
HL-60	0.185	0.468	1.824	693
Caki-1	0.001	0.474	1.658	522
OVCAR-8	−0.111	0.479	1.567	736
MOLT-4	0.268	0.481	1.950	846
LOX	0.071	0.482	1.760	875
UO-31	−0.200	0.486	1.500	772
NCI-H358	−0.140	0.503	1.621	812
A704	−0.026	0.537	1.853	700
EKV-X	−0.303	0.544	1.600	867
P388	0.230	0.561	2.194	896
NCI-H520	−0.089	0.570	1.906	776
MCF-7/ADR	−0.174	0.579	1.852	889
P388/ADR	−0.138	0.582	1.900	376
NCI-H322	−0.061	0.586	1.990	861
SNB-75	−0.329	0.750	2.297	625

*Data updated November 16, 1987. For references to test protocol and sources of cell lines, *see* Methods section.

tween the deltas obtained for a specified seed compound and the corresponding deltas for each of the other compounds in the data base. For a seed compound screened against a panel of 50 cell lines, the 50 deltas obtained for those cell lines are subtracted from the corresponding deltas obtained in testing the same 50 cell lines (or a subset of these lines if all 50 were not tested) against each of the other compounds in the data base. In this way, the mean graph pattern for the seed compound is sequentially compared quantitatively with all other mean graph patterns available. For each compound, two parameters are calculated: Av, which is the average difference between deltas (computed as the mean of the absolute values of the differences), and Max, which is the maximum difference observed.

The Av and the Max values are used by the COMPARE program to create a list of compounds ordered according to the similarity of their mean graph patterns to the mean graph pattern of the seed compound. The compounds are first sorted by Av values; compounds with lower Av values are ranked higher. Then compounds with the same Av values are further sorted by Max values; compounds with lower Max values are ranked higher. The purpose of creating the ordered list was to first rank the compounds by their similarity in mean graph fingerprints and then to investigate whether this similarity correlates with any other significant property common to the ranked compounds and the seed compound.

Since the meaning of the similarity in mean graph patterns was the central question, it was necessary to obtain additional information about the test compounds as well as relevant information about the seed compound. We constructed a data base of 88 test compounds suitable for this purpose and analyzed this data base with the COMPARE program. Application of the algorithm to data sets restricted to well-known or prototypical seed compounds led to intriguing results. Compounds known to be DNA binders (table 2), biological alkylating agents, or antimetabolites were grouped to a significant extent with agents having similar activity or structure.

In table 2, the seed compound was doxorubicin. The three compounds with the closest Av values were mitoxantrone, amsacrine, and acodazole. These three drugs and the seed compound are thought to be DNA binders and topoisomerase II inhibitors. The matching sequence includes taxol, rhizoxin, and then three more DNA binders (oxantrazole, bisantrene, and amonafide).

The COMPARE analysis using the alkylating agent melphalan as the seed for comparison showed a significant clustering of the known alkylating agents. Pipobroman, uracil mustard, and chlorambucil were ranked in that sequence as the closest matches to melphalan in the test set. The antimetabolite cytarabine was also used as the seed compound in a COMPARE analysis. Its close biological and structural analogue fazarabine ranked second to thioguanine in the listing.

Table 2. COMPARE pattern-recognition program: similarity of DNA binders and topoisomerase II inhibitors to doxorubicin*

Drug	NSC No.	Av	Max	No. of cell lines	Range†
Doxorubicin	123127	0.000	0.00	56	3.2
Mitoxantrone	301739	0.343	1.80	47	2.7
Amsacrine	249992	0.371	1.49	46	2.8
Acodazole	305884	0.380	1.39	36	1.6
Taxol	125973	0.387	1.57	49	2.6
Rhizoxin	332598	0.421	1.51	38	2.2
Oxantrazole	349174	0.427	2.43	36	1.2
Bisantrene	337766	0.451	1.47	47	3.1
Amonafide	308847	0.451	2.34	38	1.0
Discreet		0.455	2.46	27	2.0
Mitotane	38721	0.467	2.24	48	1.6
Merbarone	336628	0.486	2.33	35	0.9
10-Hydroxycamptothecin	107124	0.487	2.23	25	2.7
Dacarbazine	45388	0.491	2.02	48	2.0
Pyrazine diazohydroxide	361456	0.492	2.23	39	0.6
Spiromustine	172112	0.494	2.64	40	1.6
Busulfan	750	0.504	2.16	48	1.7
Hexamethylenebisacetamide	95580	0.507	2.44	42	1.0
Carboplatin	241240	0.508	2.69	47	2.1
Teroxirone	296934	0.514	2.18	40	1.9
Hepsulfam	329680	0.520	2.49	38	2.2
Ebifuramin	201047	0.525	2.26	36	0.6
Pyrazole	45410	0.534	2.12	41	1.0
Pipobroman	25154	0.535	3.28	48	2.8
Phyllanthoside	328426	0.537	1.82	37	3.4

*Of 88 compounds tested, these 25 were most similar to doxorubicin in this analysis of differential growth inhibition.

†Range = No. of log units between values for most sensitive and least sensitive cell lines.

There is an important caveat that applies to our algorithm. The algorithm must give a "best match" whether or not a meaningful one exists in the data base, and thus, unrelated compounds are sometimes given a high ranking. Despite this caveat, it seems that the observed mean graph patterns express valuable information, sometimes reflecting similarities in biological properties and/or chemical structure and properties. Expression of such similarities in the mean graphs appears to be sufficiently robust that this relatively simple algorithm of the COMPARE program can successfully detect and rank these similarities in an order that seems to have an exploitable degree of correlation with independently derived rankings of similarity based on biochemical and/or structural considerations.

Conclusions

We have developed a set of computerized procedures to facilitate the detection, ranking, display, and analysis of patterns of differential growth inhibition. These procedures are conceptually centered in the mean graph, which was designed to graphically represent screening results for individual compounds tested against large numbers of tumor cell lines. Experimental applications of the COMPARE program to a limited data base accrued from the pilot screen suggest the possibility of meaningful clustering of mean graph patterns that is related to biological properties and/or chemical structure and properties. The potential wealth of information to be generated in the course of the new NCI drug-screening experiment can be subjected to a wide variety of analytical procedures. Our work represents only the first of many potential avenues to data display and analysis that may be explored in the course of this project.

References

(1) BOYD MR, SHOEMAKER RH, MCLEMORE TL, ET AL: Drug development. *In* Thoracic Oncology (Roth JA, Ruckdeschel JC, Weisenburger TH, eds). Philadelphia: Saunders. In press

(2) ALLEY MC, SCUDIERO DA, MONKS A, ET AL: Feasibility of drug screening with panels of human tumor cell lines using a microculture tetrazolium assay. Cancer Res 48:589-601, 1988

(3) SCUDIERO D, SHOEMAKER RH, PAULL KD, ET AL: Evaluation of a soluble tetrazolium/formazan assay for cell growth and drug sensitivity in culture using human and other tumor cell lines. Cancer Res 48:4827-4833, 1988

(4) SHOEMAKER RH, MONKS A, ALLEY MC, ET AL: Development of human tumor cell line panels for use in disease-oriented drug screening. *In* Prediction of Response to Cancer Chemotherapy (Hall T, ed). New York: Alan R Liss, 1988, pp 265-286

(5) PAULL KD, HODES L, PLOWMAN J, ET AL: Reproducibility and response patterns of the IC50 values and relative cell line sensitivities from the NCI human tumor cell line drug screening project. Proc Am Assoc Cancer Res 29:488, 1988